

SUBREFLECTOR AND FEED SCATTERING EFFECTS IN DUAL-SHAPED REFLECTOR COMPACT RANGES[†]

William Imbriale and Victor Galindo-Israel
JPL-Caltech, Pasadena, CA 91109

Raj Mittra
Univ. of Ill., Urbana, IL 61801

I. Introduction

In a dual reflector compact range, the objective is to obtain as large a zone as possible near the main reflector where the field is planar and has minimum ripple. The contributions to phase and amplitude ripple come primarily from main reflector aperture distribution variations which can and have been reduced by appropriate aperture distribution shaping [1], and/or serrating or rolling [2], of the main reflector edge. The subreflector diffraction scattering onto the main reflector was accounted for in the analysis of an offset dual-shaped reflector pair presented in an earlier paper [1]. This was significant for the single chamber geometries. However, the feed fields and the diffraction scattering from the subreflector into the measurement zone was not accounted for in the single chamber geometry. In this paper, we extend the analysis presented earlier [1] by accounting more accurately for the feed and subreflector scattering into the measurement zone.

In a recent paper [3], scattering from the subreflector edges onto the main reflector (and into the measurement zone for single chamber geometries) was reduced by serrating the edge of the subreflector. An alternative method of reducing the effects of the subreflector edge currents is to reduce the edge illumination of the subreflector by the feed. For dual-shaped reflectors this is not difficult since the same main reflector aperture distribution can be achieved with a very wide variation of feed patterns. The principal difficulty here is to use a sufficiently good feed wherein the wide angle phase pattern is spherical and the wide angle amplitude pattern is monotonically decreasing. Usually a corrugated horn will give good results for wide angles.

In what follows, we consider three analytical feed horns of the $\cos^N(\theta)$ type wherein N is chosen in order to achieve a specified subreflector edge taper at the edge half cone angle θ_M . We choose edge tapers of -30 dB, -20 dB and -10 dB. Three different reflector profiles are then synthesized with the same geometrical optics (GO) aperture distribution and diffraction analyzed at various positions in the measurement zone of the compact range. Field computational results are compared with and without the feed and subreflector scattered fields added into the computations at the observation points in the measurement zone.

II. Dual-Shaped Reflector Geometries

Figure 1 illustrate profiles of the dual-shaped geometry of the -30 dB subreflector edge taper (at $\theta_M = 16$ degs) in the plane of symmetry. The geometries for the -20 dB and -10 dB cases differ very little except that the caustic geometry between the reflector becomes smaller in extent. The aperture distributions and other initial conditions remain the same for all three cases.

The Gregorian subreflector tilt angle, Ω , is adjusted in each case so as to minimize the cross-pol in the main reflector aperture. Cross-pol levels were in the neighborhood of -45 to -55 dB in the measurement zone. The tilt angle is also chosen so that spillover from the feed contributes very little to the fields in the measurements zone.

[†]The research described in this paper was carried out at JPL-Caltech under a contract with the National Aeronautics and Space Administration and the National Science Foundation.

III. Diffraction Analysis Results

The three dual-shaped reflector geometries were diffraction analyzed at 3 GHz so that the diameter of the main reflector (6 meters) was 60 wavelengths. The incident field was X-polarized. A physical optics algorithm was used for the main reflector while a GTD algorithm was used for the subreflector scattering. Although the physical optics and the GTD scattering from the subreflector differed very little in the measurements zone, the GTD gave a more conservative result (slightly higher scattering)—see Figure 1a. For each case that was analyzed, the results for the field in the measurement zone are presented with both the subreflector and feed fields added to the fields scattered from the main reflector as well as with these fields not added to the main reflector scattered fields. In all cases, the diffracted, not simply the GO, fields from the subreflector are used to obtain the currents on the main reflector.

In Figure 2, the amplitude of the scattered field results are presented for a cut at $Z = 8$ meters with $\rho = -3$ to $\rho = +3$ mtrs. Results are presented for feeds with a -30 dB, -20 dB, and -10 dB taper at the subreflector edge. Note that the rapid oscillations resulting from interference between the subreflector and main reflector currents is greater in magnitude in the region $\rho = 0$ to 3 mtrs—closer to the subreflector caustic. The scattered field phase results for the same cuts are presented in Figure 3.

In Figures 4 and 5, field computational results are presented for cuts at $Z = 6$ mtrs and for $Z = 10$ mtrs in the measurements zone. The interference ripple decreases markedly with increasing Z distance. This is due to the fact that the field contribution from the subreflector scattering and the feed decays roughly as $1/R$ ($R =$ approximate distance from the caustic current sources—see Figure 1), whereas the field contribution from the main reflector is **focussed as a plane wave** and does not decay with Z distance.

We have thus demonstrated that in dual-shaped reflector compact range systems, the edge taper on the subreflector can be reduced—without affecting performance—such that subreflector diffraction scattered fields contribute very little to the measurement zone ripple. This can be done **in addition** to serrating the edge of the subreflector, if desired. In general, the -20 dB and -30 dB edge tapers prove sufficient to result in virtually no interference ripple of the feed or subreflector fields anywhere in the measurement zone. The -10 dB subreflector edge taper does result in moderately substantial extra ripple effect close in to the main reflector region of the measurement zone.

III. References

- [1] V. Galindo-Israel, S. Rengarajan, W. Imbriale, and R. Mittra, "Offset dual-shaped reflectors for dual chamber compact ranges," *IEEE Trans. Antennas Propagat.*, vol. AP-39, pp. 1007–1013, Mar. 1989.
- [2] C. W. Pistorius, C. G. Clerici, and W. D. Burnside, "A Dual Chamber Gregorian subreflector system for compact range applications," *IEEE Trans. Antennas Propagat.*, vol. AP-37, pp. 342–347, Mar. 1989.
- [3] I. J. Gupta, D. G. Brown, W. D. Burnside, and W. Lin, "A serrated edge Gregorian subreflector for dual chamber compact range systems," *IEEE Trans. Antennas Propagat.*, vol. AP-39, pp. 1258–1261, Aug. 1991.

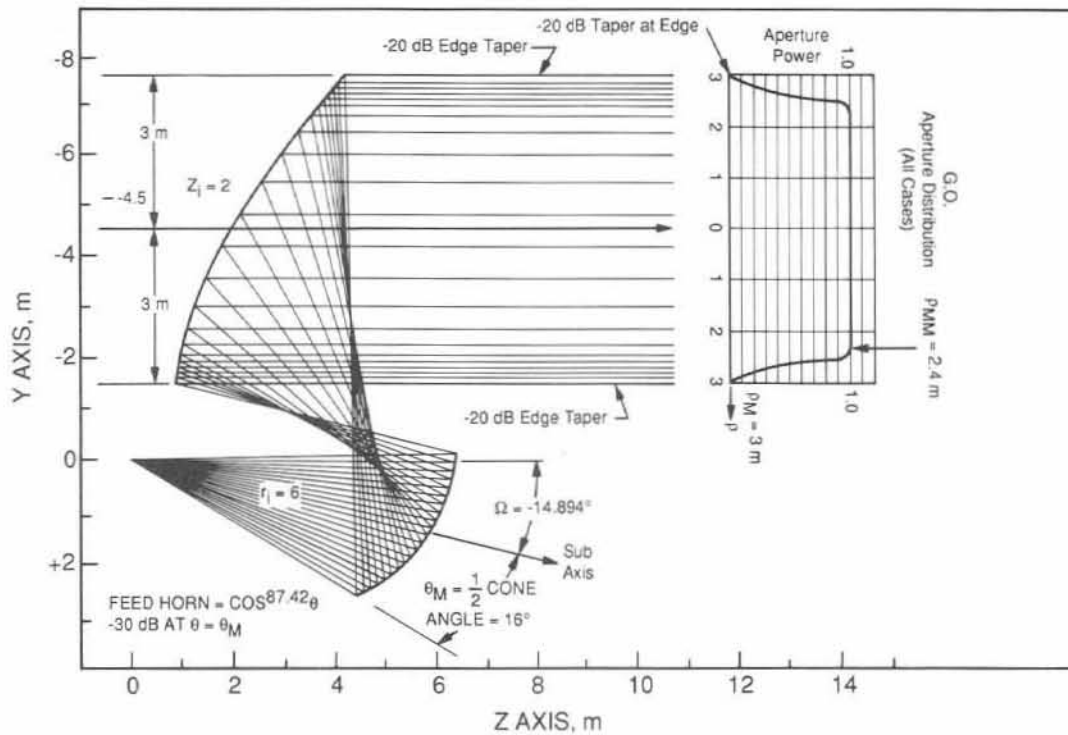


Figure 1. Dual-Shaped Reflectors with -30 dB Edge Taper Feed

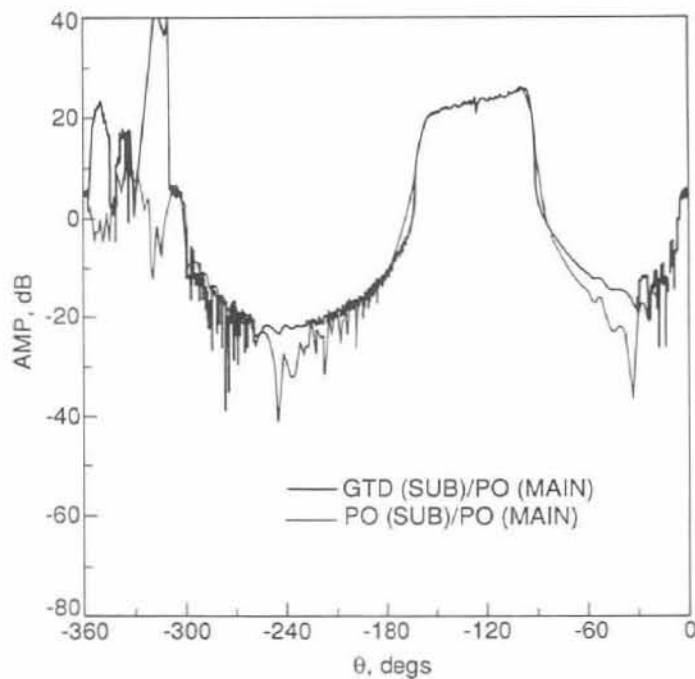


Figure 1a. Circular Cut in Offset Plane (Y-Z Plane) at $R = 7.25$ Meters Centered at Caustic of -20 dB Edge Taper Design. $D = 60 \lambda$, Polarization = X Directed.

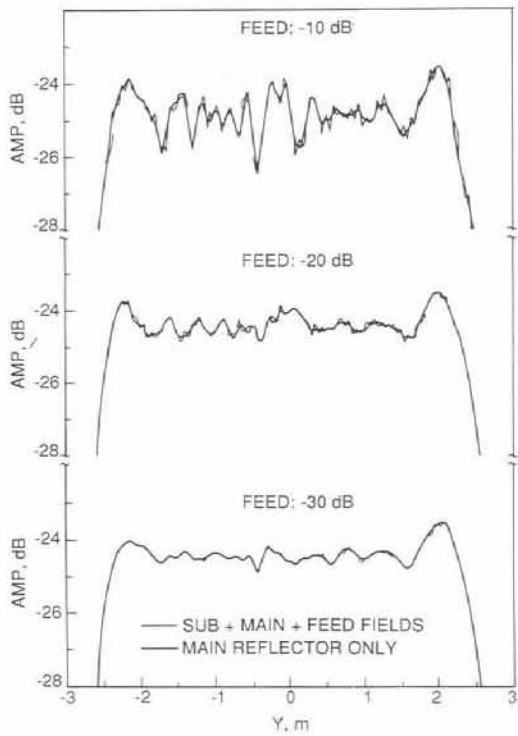


Figure 2. Cut at Z = 8 mtrs. GTD/PO Analysis. $D = 60 \lambda$, Polarization: X-Linear.

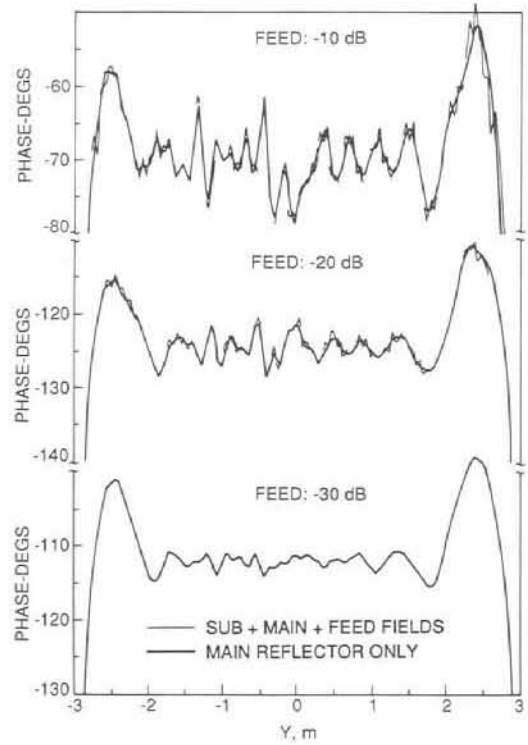


Figure 3. Phase Cuts. Cut at Z = 8 mtrs. GTD/PO Analysis. $D = 60 \lambda$, Polarization: X-Linear.

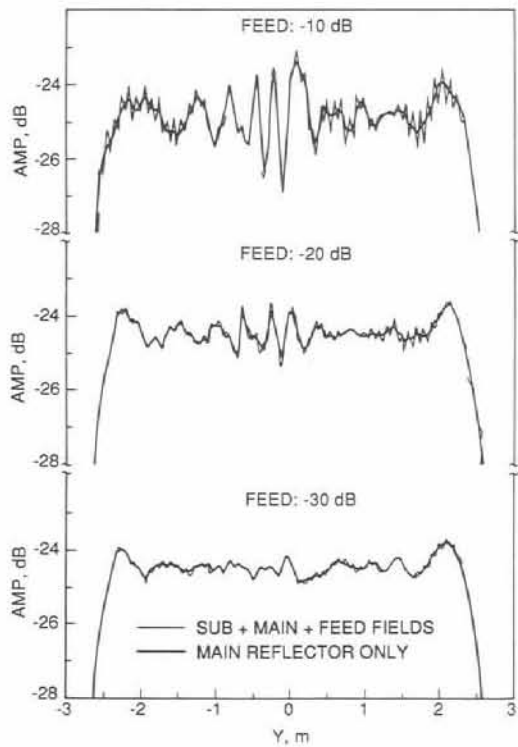


Figure 4. Cut at Z = 6 mtrs. GTD/PO Analysis. $D = 60 \lambda$, Polarization: X-Linear.

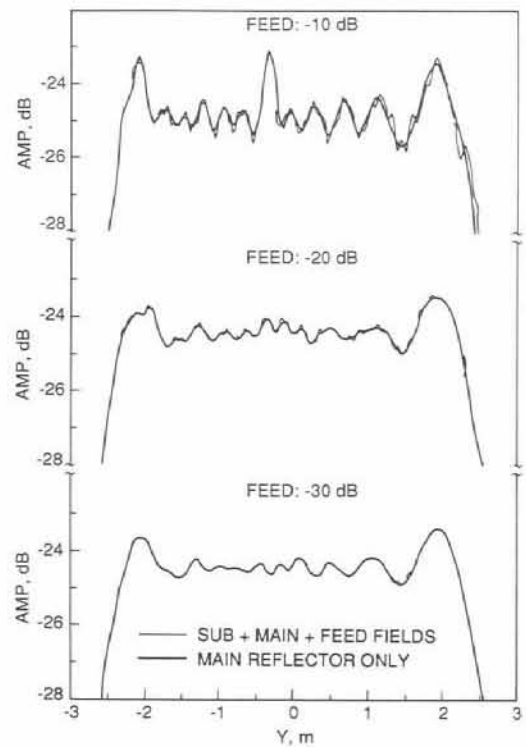


Figure 5. Cut at Z = 10 mtrs. GTD/PO Analysis. $D = 60 \lambda$, Polarization: X-Linear.